

# Two-dimensional solitons in saturable media with a quasi-one-dimensional lattice potential

Thawatchai Mayteevarunyoo

*Department of Telecommunication Engineering, Mahanakorn University of Technology, Bangkok 10530, Thailand*

Boris A. Malomed

*Department of Interdisciplinary Studies, School of Electrical Engineering, Tel Aviv University, Tel Aviv 69978, Israel*

(Received 19 November 2005; published 22 March 2006)

We study families of solitons in a two-dimensional model of the light transmission through a photorefractive medium equipped with a (quasi-)one-dimensional photonic lattice. The soliton families are bounded from below by finite minimum values of the peak and total power. Narrow solitons have a single maximum, while broader ones feature side lobes. Stability of the solitons is checked by direct simulations. The solitons can be set in motion across the lattice (actually, made tilted in the spatial domain), provided that the respective boost parameter does not exceed a critical value. Collisions between moving solitons are studied too. Collisions destroy the solitons, unless their velocities are sufficiently small. In the latter case, the colliding solitons merge into a single stable pulse.

DOI: [10.1103/PhysRevE.73.036615](https://doi.org/10.1103/PhysRevE.73.036615)

PACS number(s): 42.65.Tg, 42.70.Nq

## I. INTRODUCTION

As was first predicted in Ref. [1], a periodic lattice potential induced in a photorefractive medium, which is characterized by the saturable nonlinearity, may be an efficient tool for creation and stabilization of two-dimensional (2D) spatial solitons of various types. The prediction was followed by the experimental observation of ordinary solitons [2], localized vortices with the topological charge 1 belonging to the first (lowest) [3] or second [4] bandgap in the respective linear spectrum (stable higher-order vortices and *supervortices* in such systems were recently predicted too [5]), dipole- and quadrupole-mode solitons [6], steady patterns in the form of soliton necklaces [7], and some others. A review of the field was recently given in Ref. [8].

In the experiment, the periodic potential is induced by the photonic lattice, which is created as a superposition of counterpropagating laser beams illuminating the photorefractive crystal in the ordinary polarization, in which the light propagation is nearly linear; then, the spatial solitons are built in a probe beam launched through the lattice in the extraordinary polarization (i.e., polarized along the crystalline  $c$  axis), which is subject to strong nonlinearity induced by the dc bias electric field applied to the crystal [1,8]. Using this technique, the square photonic lattice can be created by two pairs of counterpropagating beams illuminating the crystal in directions orthogonal to each other and to the probe beam that gives rise to the soliton(s).

On the other hand, 2D solitons can also be supported by a low-dimensional, i.e., quasi-one-dimensional (Q1D) periodic potential, that may be readily induced by a single pair of counterpropagating beams illuminating the bulk crystal in the ordinary polarization. Recently, it has been predicted that the Q1D lattice may efficiently stabilize 2D solitons in the model with the cubic (rather than saturable) nonlinearity [9]. This result directly applies to Bose-Einstein condensates with attractive interactions between atoms, trapped in a photonic lattice; moreover, it has also been demonstrated [9,10] that a quasi-2D lattice can stabilize three-dimensional (3D)

solitons against strong collapse that the cubic nonlinearity gives rise to in the latter case. Two-dimensional solitons supported by the Q1D lattice naturally demonstrate strong anisotropy, which makes them essentially different from the usual 2D solitons. A significant advantage offered by the use of the Q1D lattice is the fact that the remaining free direction allows the solitons to move (in the spatial domain, “motion” means a tilt of the soliton beam), which opens a way to study collisions between them, formation of bound states, etc. [9]. The mobility of 2D solitons may also be strongly anisotropic in some 2D lattices [11].

The objective of the present work is to introduce 2D solitons in the model of the photorefractive media with the saturable nonlinearity and Q1D periodic potential (Q1D solitons—which are, effectively, one-dimensional objects—in the model of the 2D photorefractive medium with the Q1D lattice were introduced in Ref. [12]). The soliton solutions are constructed in Sec. II. We demonstrate that the Q1D solitons are characterized by minimum peak and total intensities necessary for their existence, and they are stable in the entire existence region. Moving solitons and collisions between them are studied in Sec. III. We find that collisions destroy the solitons, unless the collision “velocity” (in fact, the relative tilt of the two spatial solitons) is small enough; in the latter case, the colliding solitons merge into a single soliton, irrespective of the orientation of the velocity vector relative to the Q1D lattice.

The model outlined above is based on an equation for the spatial evolution of the probe field (the slowly varying amplitude  $U$  of the electromagnetic wave in the extraordinary polarization), which follows the standard description of photorefractive media [1]. In normalized units, the equation takes the form

$$i \frac{\partial U}{\partial z} + \frac{\partial^2 U}{\partial x^2} + \frac{\partial^2 U}{\partial y^2} - \frac{U}{1 + I_0 \cos^2(\pi x/d) + |U|^2} = 0, \quad (1)$$

where  $I_0$  and  $d$  are the peak intensity and period of the photonic lattice induced by the superposition of counterpropa-

gating waves launched along the  $x$  axis in the ordinary polarization. The normalized propagation and transverse coordinates,  $z$  and  $(x, y)$ , are proportional to their counterparts measured in physical units,  $Z$  and  $(X, Y)$ , so that  $z = Z / (k_0 \Delta n_0)$  and  $(x, y) = (X, Y) / \sqrt{2k_0 n_0 \Delta n_0}$ , where  $k_0$  is the propagation constant of the probe wave, and  $\Delta n_0 = n_0^3 r_{33} E / 2$  is the change of the refractive index  $n_0$  (accounted for by the electro-optic coefficient  $r_{33}$ ) caused by the dc electric field  $E$ .

## II. TWO-DIMENSIONAL SOLITONS AND THEIR STABILITY

Soliton solutions to Eq. (1) are searched for as

$$U = u(x, y) e^{-i\mu z}, \quad (2)$$

where  $-\mu$  is the shift of the propagation constant in the soliton, and the real function  $u$  satisfies the equation

$$\frac{\partial^2 u}{\partial x^2} + \frac{\partial^2 u}{\partial y^2} + \left[ \mu - \frac{1}{1 + I_0 \cos^2(\pi x/d) + u^2} \right] u = 0. \quad (3)$$

Solutions  $u(x, y)$  of this equation were found by means of an iteration procedure in the Fourier space. To this end, following a numerical method elaborated in Ref. [6], Eq. (3) was rewritten for the Fourier transform  $\hat{u}(k_x, k_y)$  in the form

$$\hat{u} = \frac{1}{k_x^2 + k_y^2 - \mu + 1} \left\{ \mathcal{F} \left( \frac{I_0 \cos^2(\pi x/d) u}{1 + I_0 \cos^2(\pi x/d) + |u|^2} \right) + \mathcal{F} \left( \frac{|u|^2 u}{1 + I_0 \cos^2(\pi x/d) + |u|^2} \right) \right\}, \quad (4)$$

$\mathcal{F}(\dots)$  standing for the 2D Fourier transform. A direct iteration procedure applied to Eq. (4) does not converge, in the general case. Therefore, the equation was modified. Defining integral factors:

$$\alpha = \int \int \left\{ (k_x^2 + k_y^2 - \mu + 1) \hat{u} - \mathcal{F} \left( \frac{I_0 \cos^2(\pi x/d)}{1 + I_0 \cos^2(\pi x/d) + |u|^2} u \right) \right\} \hat{u}^* dk_x dk_y, \quad (5)$$

$$\beta = \int \int \mathcal{F} \left( \frac{|u|^2 u}{1 + I_0 \cos^2(\pi x/d) + |u|^2} \right) \hat{u}^* dk_x dk_y, \quad (6)$$

where  $*$  stands for the complex conjugation, the following iterative equation was introduced,

$$\hat{u}_{n+1} = \frac{1}{k_x^2 + k_y^2 - \mu + 1} \times \left\{ \left( \frac{\alpha_n}{\beta_n} \right)^{1/2} \mathcal{F} \left( \frac{I_0 \cos^2(\pi x/d)}{1 + I_0 \cos^2(\pi x/d) + |u_n|^2} u_n \right) + \left( \frac{\alpha_n}{\beta_n} \right)^{3/2} \mathcal{F} \left( \frac{|u_n|^2 u_n}{1 + I_0 \cos^2(\pi x/d) + |u_n|^2} \right) \right\}, \quad (7)$$

where  $\alpha_n$  and  $\beta_n$  are the factors (5) and (6) corresponding

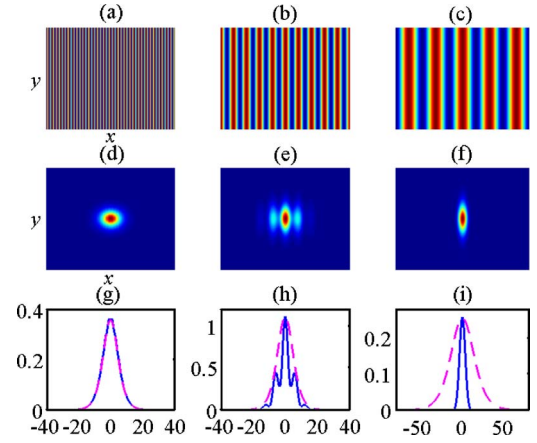


FIG. 1. (Color online) Typical examples of two-dimensional solitons found from Eq. (3) with a moderately strong quasi-one-dimensional photonic lattice, corresponding to  $I_0 = 5$ . Panels (a)–(c) show the intensity distribution in the photonic lattice,  $I_{\text{phl}}(x) = I_0 \cos^2(\pi x/d)$ , for  $d = \pi/5$ ,  $2\pi$ , and  $10\pi$ , respectively. The two-dimensional intensity field in the respective solitons is shown in panels (d)–(f), and the corresponding intensity profiles in two cross sections of the solitons, along  $y=0$  and  $x=0$ , are displayed in panels (g)–(i) by continuous and dashed lines, respectively.

to the function  $\hat{u}_n$ . Fixed points of Eq. (7), corresponding to  $\lim_{n \rightarrow \infty} (\alpha_n / \beta_n) = 1$ , yield solutions to Eq. (4) as well. The iterative procedure based on Eq. (7) provides for fast convergence, and produces solutions displayed below.

Typical examples of the 2D solitons are shown in Fig. 1. In particular, the picture observed in the left column of the figure is typical to cases when the lattice potential is weak, and/or the soliton's peak intensity essentially exceeds the lattice's amplitude  $I_0$ : the soliton is practically isotropic, without a conspicuous effect of the lattice. The picture in the right column is typical for a relatively strong lattice with a large period: then, the soliton is almost entirely trapped in one potential trough, assuming an elliptic shape. In either case, the soliton's shape features a single lobe, either circular or elliptic one.

The most interesting case is represented by the central column in Fig. 1, which demonstrates a soliton with well-pronounced side lobes in a moderately strong lattice (in physical units, this case corresponds to typical values of parameters available in the experiment). Naturally, the multi-humped structure is observed only along the axis  $x$ , while in the free direction,  $y$ , the soliton always features a simple single-hump form. Results reported below are given for the same period,  $d = 2\pi$ , which gives rise to the central column in Fig. 1. For other values of  $d$  which are neither very small nor very large, the results are quite similar.

The solitons are characterized by the peak intensity (power),  $I_p \equiv |u(x=0, y=0)|^2$ , and integral intensity,

$$P \equiv \int_{-\infty}^{+\infty} \int_{-\infty}^{+\infty} |u(x, y)|^2 dx dy. \quad (8)$$

Accordingly, soliton families for given values of  $I_0$  and  $d$  are represented by the dependences  $P(\mu)$  and  $I_p(\mu)$ , see Fig. 2

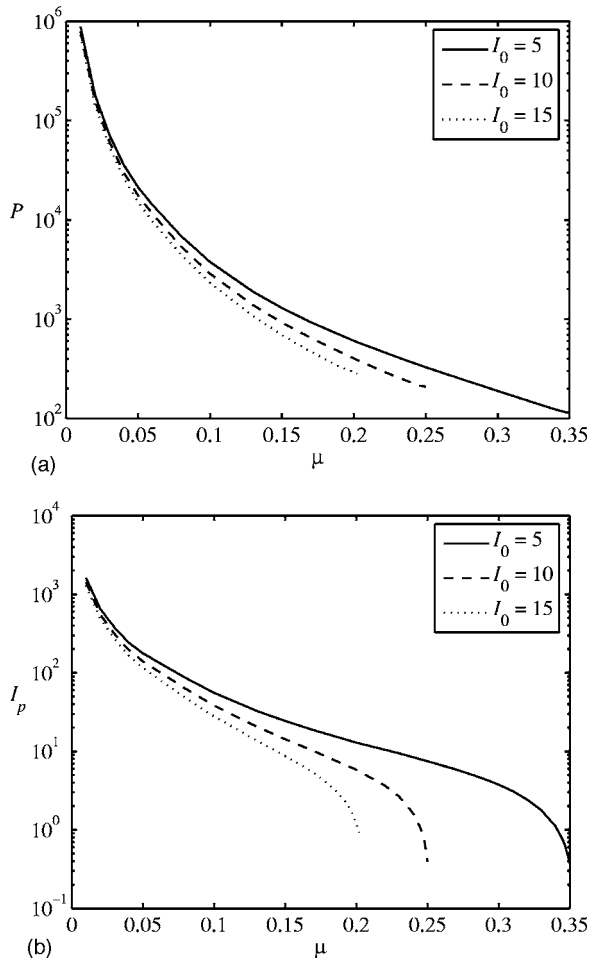


FIG. 2. The total intensity (power) (a) and peak intensity (b) of families of two-dimensional solitons vs the absolute value of the propagation-constant shift,  $\mu$ , for  $d=2\pi$ , and different values of the photonic-lattice strength,  $I_0$ . The curves terminate at points where the solitons cease to exist.

[recall  $-\mu$  is the soliton propagation-constant shift, defined in Eq. (2)]. An important feature observed in this figure is that the 2D solitons exist, with a given lattice strength  $I_0$ , only for  $P$  and  $I_p$  exceeding certain finite minimum (threshold) values,  $P_{\min}$  and  $I_{p,\min}$ ; for instance,  $I_{p,\min}=0.0411$  for  $I_0=5$  and  $d=2\pi$ . Both minimum values are shown, as functions of the strength  $I_0$  of the photonic lattice, in Fig. 3. It should be noticed that a lower intensity threshold necessary for the existence of 2D solitons in models combining lattice potentials with various nonlinearities was found in earlier works [1,9,13].

It is easy to check that the soliton families shown in Figs. 1 and 2 belong to the semi-infinite bandgap in the spectrum of the linearized equation (1). It is known that, on top of the semi-infinite gap, a sufficiently strong lattice may give rise to solitons in finite bandgaps of models combining a periodic potential and saturable nonlinearity (see, e.g., Ref. [14]). In this work, we do not aim to look for gap solitons of such types.

Proceeding to the investigation of stability of the 2D solitons, we first of all note that the negative slope of the dependence  $P(\mu)$ , obvious in Fig. 2, suggests possible stability of

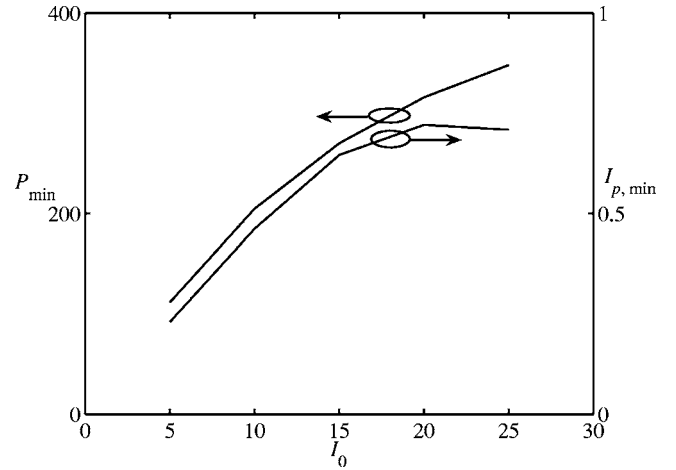


FIG. 3. The minimum peak intensity,  $I_{p,\min}$ , and total power,  $P_{\min}$ , necessary for the existence of the two-dimensional solitons vs the strength,  $I_0$ , of the underlying quasi-one-dimensional lattice.

the soliton families pursuant to the Vakhitov-Kolokolov (VK) criterion [15], which may guarantee the absence of unstable modes of small perturbations corresponding to real eigenvalues of the instability growth rate. The full stability is not provided by the VK criterion, and, moreover, the applicability of the criterion even to perturbations with real eigenvalues was not proven in the present context. In fact, a counterexample is known: soliton subfamilies which should be VK-unstable in a 1D model combining a periodic potential of the Kronig-Penney type and cubic-quintic nonlinearity (another variety of the saturation) were found to be *completely stable* [14].

We have tested stability of the 2D solitons in direct simulations of Eq. (1), making use of the fast Fourier transform in directions  $x$  and  $y$  and Runge-Kutta method to advance in  $z$ . In each simulation, some amount of random noise was added to the soliton as a perturbation. It has been concluded that *all the solitons* are stable, as (formally) predicted by the VK criterion. An example illustrating the stability of a large-amplitude 2D soliton with  $I_0=5$  and  $I_p=56.76$  is displayed in Fig. 4(a). Broad solitons, with the peak intensity close to the threshold value  $I_{p,\min}$ , are stable too, although their peak intensity may slowly grow with  $z$ , as shown in Fig. 4(b) for the same lattice strength,  $I_0=5$ , as in Fig. 4(a), but  $I_p=1.1$ . A plausible explanation to the latter effect is that the combination of the lattice potential and self-focusing nonlinearity (for relatively small  $I_p$ , the saturation does not suppress the self-focusing) leads to sucking the perturbation wave field into the spot where the soliton's maximum is located, and the buildup of the additional wave field around the soliton's peak may be conspicuous, against the backdrop of the relatively small value of  $I_p$ .

### III. MOVING TWO-DIMENSIONAL SOLITONS AND THEIR COLLISIONS

Solutions  $\tilde{U}(x,y,z)$  for solitons “moving” (actually, tilted) along the free direction  $y$  can be generated from the “quies-

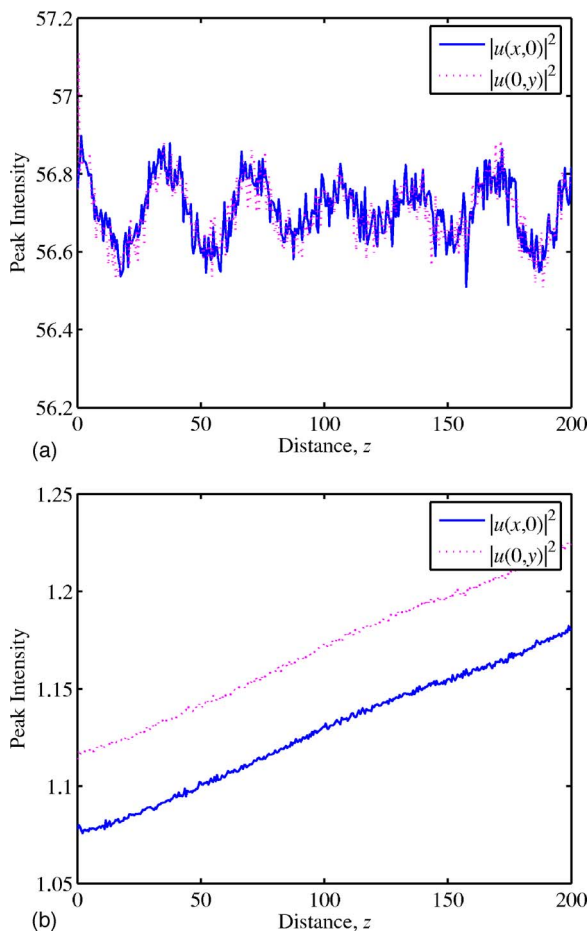


FIG. 4. (Color online) (a) Stable evolution of a high-intensity soliton, with  $I_0=5$  and  $I_p=56.76$ , under random perturbations, is illustrated by the  $z$  dependence of the soliton’s peak intensity. (b) The same for a low-intensity soliton, with  $I_p=1.1$ .

cent” solitons reported in the previous section,  $U(x,y,z)$ , by means of the Galilean transformation,

$$\tilde{U}(x,y,z) = U(x,y - 2Q_y z, z) \exp(iQ_y x - iQ_y^2 z), \quad (9)$$

where  $Q_y$  is an arbitrary *boost parameter*, that determines the soliton’s “velocity” (tilt)  $2Q_y$ . On the other hand, generation of solitons tilted along the  $x$  axis is a nontrivial problem. In the 1D version of Eq. (1), without the term  $\partial^2 U / \partial y^2$ , a family of tilted solitons was introduced in Ref. [12].

We looked for solitons “moving” along the  $x$  axis by simulating the evolution of initial states of the form

$$U_0(x,y) = U(x,y) \exp(iQ_x x), \quad (10)$$

cf. Eq. (9), where  $U(x,y)$  corresponds to a zero-velocity stationary soliton solution. The boost parameter in Eq. (10),  $Q_x$ , was gradually increased from a run to a run, until reaching a critical (maximum) value  $Q_{\max}$ , at which the initial configuration (10) does not generate any soliton, but rather gets destroyed into small-amplitude waves. Results of the simulations are summarized in Fig. 5, in the form of plots showing  $Q_{\max}$  as a function of the soliton’s peak intensity  $I_p$ , for different values of the lattice strength  $I_0$ . Measurement of the

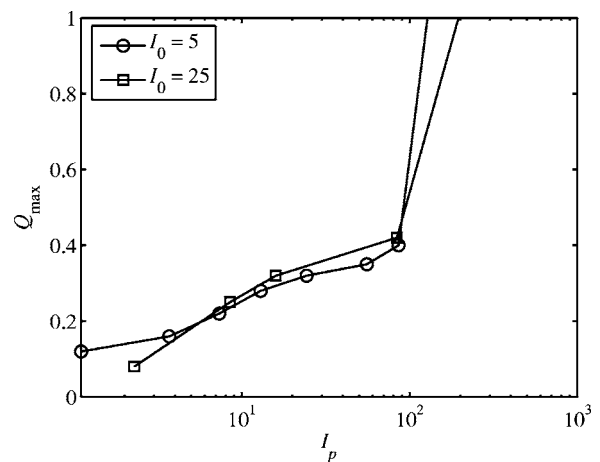


FIG. 5. The maximum value of the boost parameter,  $Q_x$ , which generates solitons moving (actually, tilted in the spatial domain) along the  $x$  axis vs the soliton’s peak intensity,  $I_p$ , for different value of the strength  $I_0$  of the underlying lattice. For  $Q_x > Q_{\max}$ , the application of the boost destroys the soliton.

established value of the average “velocity” (tilt) of the solitons generated by the initial condition (10) with  $Q_x < Q_{\max}$  produces values which are quite close to ones ( $2Q_x$ ) corresponding to the Galilean transform (9) in the free space. Finally, applying the Galilean transformation (9) to the soliton already moving along the  $x$  direction, one can generate a pulse moving in any direction (in particular, along the diagonal,  $x=y$ , see below).

Once the stability limits for the moving solitons are available, the next step is to consider collisions between them. The outcome of the collision may depend on the magnitude and direction of the velocities, and the aiming mismatch (its zero value corresponds to the head-on collision).

Numerous simulations demonstrate that the collision completely destroys both solitons, unless their velocities are sufficiently small. An example of the destructive collision is displayed in Fig. 6. In particular, in the case of  $I_0=5$ , the solitons must not be set in motion by the boost with  $|Q_x|$

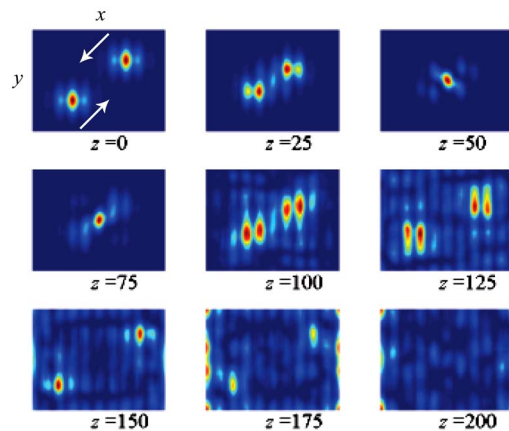


FIG. 6. (Color online) A typical example of destructive collisions between moving solitons, for  $I_0=5$  and  $I_p=1.78$ . The velocity vectors of the colliding solitons (shown by arrows in the first panel, in this figure and in Fig. 7) have components  $Q_{x,y} = \pm 0.12$ .

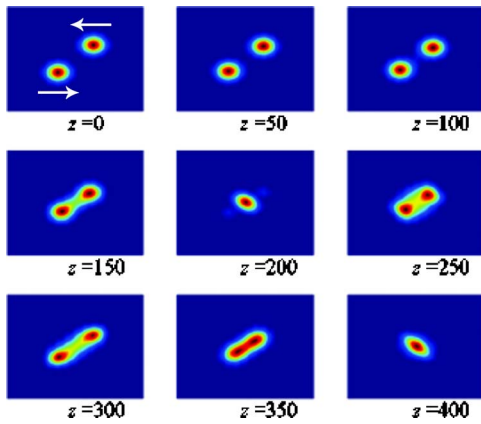


FIG. 7. (Color online) Merger of colliding solitons which were set in motion by the boost  $Q_x = \pm 0.01$ , with a finite aiming mismatch in the  $y$  direction. In this case,  $I_0 = 25$  and  $I_p = 83.97$ .

or  $|Q_y|$  in excess of 0.05, otherwise the collision will destroy them. This critical value is the same for the motion in the  $x$  and  $y$  directions, up to the accuracy of the simulations. Moreover, if the solitons are boosted in the diagonal direction and then collide, the same limit,  $|Q| = 0.05$ , was found for the absolute value of the corresponding vectorial boost,  $|Q| = \sqrt{Q_x^2 + Q_y^2}$ , i.e., the critical boost is virtually isotropic.

Collisions between solitons boosted by  $|Q|$  with values smaller than the critical one result in their *merger* into a single pulse. An example of the merger resulting from the collision with a finite aiming mismatch is displayed in Fig. 7. Further, the mergers caused by head-on collisions in the diagonal or vertical ( $y$ ) direction are presented in Fig. 8. As seen from the figures, the pulse generated by the merger performs intrinsic vibrations, but remains stable.

The above examples displayed collisions of single-lobe solitons. Collisions between their broader counterparts, which feature side lobes in the  $x$  direction, are quite similar. Figure 9 presents an example of the head-on collision between sufficiently slowly moving solitons of the latter type. The collision again leads to the merger of the pulses into a single pulse, which then performs conspicuous intrinsic vibrations, but remains a stable object. Additional simulations show that the soliton produced by the merger of two multi-lobe solitons can also easily move across the lattice, if given a push.

Thus we conclude that collisions between the 2D solitons are always *strongly inelastic* (both the destruction and merger of the colliding solitons are inelastic outcomes), attesting to the fact that the present model is far from any integrable limit, where collisions between solitons would be elastic. For comparison, we note that the collisions may be less inelastic in the 2D model with the Q1D periodic potential if the nonlinearity is cubic [9]. In that model, elastic collisions are possible (passage of the solitons in the case of a finite aiming mismatch, or their mutual bounce after the head-on collision, if the phase shift between them is  $\pi$ ). An additional inelastic outcome of the head-on collisions between in-phase 2D solitons, which was observed in the model with the cubic nonlinearity, but

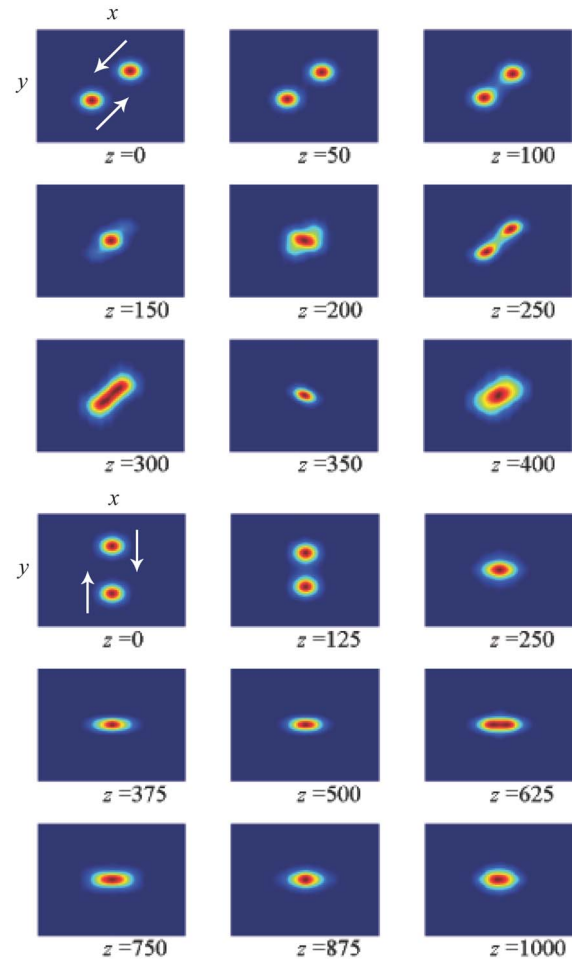


FIG. 8. (Color online) Merger as a result of head-on collisions between slowly moving solitons that were set in motion (a) along the diagonal direction, by the application of the boost with  $Q_x = Q_y = \pm 0.01$ , and (b) in the vertical direction, by the boost  $Q_y = \pm 0.01$ . In case (a),  $I_0 = 25$  and  $I_p = 83.97$ ; in case (b),  $I_0 = 15$  and  $I_p = 27.92$ .

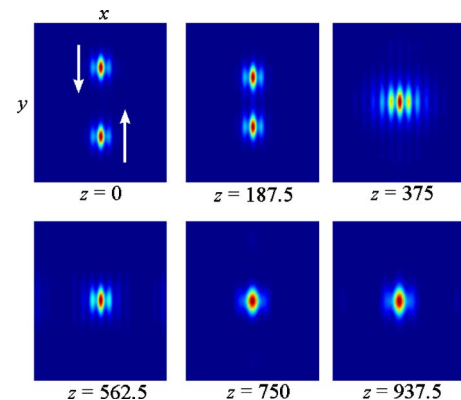


FIG. 9. (Color online) Merger of broad (multilobed) solitons caused by the head-on collision. The solitons were set in motion by the vertical boost with  $Q_y = \pm 0.01$ . In this case,  $I_0 = 5$  and  $I_p = 1.786$ .

cannot occur if the nonlinearity is saturable, is collapse of the single pulse formed after the merger of two solitons (i.e., formation of a singularity after a finite propagation distance).

#### IV. CONCLUSION

In this paper, we have proposed a model of the two-dimensional (2D) medium with the saturable nonlinearity and quasi-1D lattice potential, that can be realized in the spatial domain in a bulk photorefractive crystal. The subject of the analysis was 2D solitons (ones belonging to the semi-infinite bandgap in the linear spectrum). It was demonstrated that they form families bounded from below by finite mini-

um values of the peak and total intensities. Narrow pulses feature a single maximum, while broad solitons contain side lobes. Direct simulations confirm that the solitons are stable. They can be set in motion (actually, tilted in the spatial domain) in an obvious way along the quasi-1D lattice, and also across the lattice, provided that, in the latter case, the boost parameter does not exceed a critical value, beyond which the soliton is destroyed.

Collisions between stable moving solitons were studied in detail, with the conclusion that the collisions destroy the solitons, unless their velocities are sufficiently small. In the latter case, the colliding solitons merge into a single stable pulse that performs intrinsic vibrations. The predictions reported in this paper can be readily implemented experimentally in photorefractive crystals.

- 
- [1] N. K. Efremidis, S. Sears, D. N. Christodoulides, J. W. Fleischer, and M. Segev, *Phys. Rev. E* **66**, 046602 (2002); N. K. Efremidis, J. Hudock, D. N. Christodoulides, J. W. Fleischer, O. Cohen, and M. Segev, *Phys. Rev. Lett.* **91**, 213906 (2003).
- [2] J. W. Fleischer, M. Segev, N. K. Efremidis, and D. N. Christodoulides, *Nature* **422**, 147 (2003); J. W. Fleischer, G. Bartal, O. Cohen, O. Manela, M. Segev, J. Hudock, and D. N. Christodoulides, *Phys. Rev. Lett.* **92**, 123904 (2004).
- [3] D. N. Neshev, J. Alexander, E. A. Ostrovskaya, Y. S. Kivshar, H. Martin, I. Makasyuk, and Z. Chen, *Phys. Rev. Lett.* **92**, 123903 (2004); J. W. Fleischer, G. Bartal, O. Cohen, O. Manela, M. Segev, J. Hudock, and D. N. Christodoulides, *ibid.* **92**, 123904 (2004).
- [4] O. Manela, O. Cohen, G. Bartal, J. W. Fleischer, and M. Segev, *Opt. Lett.* **29**, 2049 (2004).
- [5] H. Sakaguchi and B. A. Malomed, *Europhys. Lett.* **72**, 698 (2005).
- [6] J. Yang, I. Makasyuk, A. Bezryadina, and Z. Chen, *Stud. Appl. Math.* **113**, 389 (2004).
- [7] J. Yang, I. Makasyuk, P. G. Kevrekidis, H. Martin, B. A. Malomed, D. J. Frantzeskakis, and Z. Chen, *Phys. Rev. Lett.* **94**, 113902 (2005).
- [8] J. W. Fleischer, G. Bartal, O. Cohen, T. Schwartz, O. Manela, B. Freedman, M. Segev, H. Buljan, and N. K. Efremidis, *Opt. Express* **13**, 1780 (2005).
- [9] B. B. Baizakov, B. A. Malomed, and M. Salerno, *Phys. Rev. A* **70**, 053613 (2004); in *Nonlinear Waves: Classical and Quantum Aspects*, edited by F. Kh. Abdullaev and V. V. Konotop (Kluwer Academic Publishers, Dordrecht, 2004), p. 61; also available at [http://rsphy2.anu.edu.au/~asd124/Baizakov\\_2004\\_61\\_NonlinearWaves.pdf](http://rsphy2.anu.edu.au/~asd124/Baizakov_2004_61_NonlinearWaves.pdf)
- [10] D. Mihalache, D. Mazilu, F. Lederer, Y. V. Kartashov, L.-C. Crasovan, and L. Torner, *Phys. Rev. E* **70**, 055603(R) (2004).
- [11] R. Fischer, D. Träeger, D. N. Neshev, A. A. Sukhorukov, W. Krolikowski, C. Denz, and Y. S. Kivshar, *Phys. Rev. Lett.* **96**, 023905 (2006).
- [12] B. A. Malomed, T. Mayteevarunyoo, E. A. Ostrovskaya, and Y. S. Kivshar, *Phys. Rev. E* **71**, 056616 (2005).
- [13] B. B. Baizakov, B. A. Malomed, and M. Salerno, *Europhys. Lett.* **63**, 642 (2003).
- [14] I. M. Merhasin, B. V. Gisin, R. Driben, and B. A. Malomed, *Phys. Rev. E* **71**, 016613 (2005).
- [15] M. G. Vakhitov and A. A. Kolokolov, *Izv. Vyssh. Uchebn. Zaved., Radiofiz.* **16**, 1020 (1973) [*Sov. J. Quantum Electron.* **16**, 783 (1973)]; see also L. Bergé, *Phys. Rep.* **303**, 260 (1998).